



DYNAMIC RESPONSE OF CURVED SURFACE SLIDER DEVICES UNDER SEVERE INPUT MOTION

M. Furinghetti ^(1,3), T. Yang ⁽²⁾, P.M. Calvi ⁽²⁾, A. Pavese ⁽¹⁾

⁽¹⁾ Department of Civil Engineering and Architecture, University of Pavia, Pavia, Italy, marco.furinghetti@unipv.it, a.pavese@unipv.it

⁽²⁾ University of Washington, Seattle, Seattle, United States, tianyy3@uw.edu, pmc85@uw.edu

⁽³⁾ EUCENTRE Foundation, Pavia, Italy

Abstract

Curved Surface Slider (CSS) devices have been widely used in recent years for the reduction of seismic vulnerability of structural systems. The most important aspects to be considered in the design phases, such as the dependence of frictional properties on parameters such as vertical load, contact pressure, temperature rise and repetition of cycles, have been identified experimentally. Based on the experimental evidence produced over the years, several analytical and numerical models have been defined and implemented that are capable of providing realistic and accurate simulations of base-isolated systems subjected to earthquake-induced ground motions. While the use of base isolation is intended to reduce the seismic vulnerability of structures, recent risk assessment studies have revealed that base isolated systems can be characterized by higher seismic risk than their “fixed-base” counterparts. However, this outcome is at least partly due to the definition of “collapse” that has traditionally been adopted for base isolated structures, which is somewhat stricter than for many other structural systems. More specifically, in most circumstances, a base isolator is assumed to collapse once the sliding pad reaches maximum displacement (that is when the pad edge reaches the edge of the sliding surface). In fact, recent studies have shown that in systems without restraining rims, higher displacements can be achieved and that the functionality of the devices can be maintained beyond their theoretical displacement capacity. The experimental program summarized in this paper analyzes the response of CSS devices under extreme seismic loading, with focus on base isolation devices stressed beyond their nominal capacity. The main response parameters of the isolation systems are analyzed in the context of both quasi-static and dynamic tests. The results collected are used to assess the behavior and effective capacity CSS devices, when design characteristics are overcome.

Keywords: Concave Surface Slider; extra-stroke; extreme loading conditions; experimental campaign; Seismic isolation.



1. Introduction

Base isolation is one of the most efficient strategies to mitigate vulnerabilities of structures during a seismic event ([3]). Among the available isolation devices, Concave Surface Slider isolators limit the seismic forces that can be transferred to the superstructure, while providing high energy dissipation capacity. This greatly reduces the overall seismic demand on the building, ensuring effective protection of both structural and non-structural elements ([2], [8], [11] and [12]). However, recent risk assessment studies have shown that, in comparison to fixed-base structures, base-isolated structures may be affected by higher vulnerability ([4]). It is believed that this somewhat surprising outcome can be (at least partly) attributed to the strict definition of collapse, that is typically adopted for base-isolated structures. To this end, base-isolated structures are assumed to collapse once the design displacement is reached at the base isolation layer. In contrast, fixed-base structures are allowed to experience displacement and forces that are beyond design limit due to ductility of the superstructure.

In fact, the results of recent experimental programs dedicated to investigating the response of CSS devices under extreme loading conditions suggest that CSS devices do not necessarily fail once the design displacement is reached. This finding extends to both CSS devices with and without restraining rims, which represent the most common mechanical configurations. According to Bao et al. 2017 ([1]), when the design displacement is reached, the impact force in bearings with bolted rims can cause substantial plastic deformation of the stopper ring. In certain cases the connecting rim bolts can be sheared, without the occurrence of significant uplift of the sliding system. On the other hand, if the rim is fully connected to the sliding surface, large uplift could occur and the restraining rim could experience large plastic deformation. Furinghetti et al. ([9]) have shown that these issues can be potentially overcome by removing the restraining rims. The main benefits of this solution include: (i) higher displacement capacity; and (ii) avoidance of impact forces upon reaching design displacement.

This paper summarizes the results of a recent experimental program conducted at the EUCENTRE Foundation Laboratory in Pavia (Italy) [13]. A series of full-scale CSS devices were tested under several input motions, with peak displacement demands exceeding the design values. The objective of this study was to investigate whether an “extra-design” displacement capacity can be considered for base-isolated structures subjected to ground motions induced by rare seismic events.

2. Tested isolation devices

The CSS devices tested in this program consist of one (Single) or two (Double) stainless steel spherical surfaces and a slider that is coated with low-friction material, such as Teflon (PTFE) or polyethylene (PE) ([5], [7]). The main properties of the base isolators considered are summarized in Table 1.

Table 1 – Devices characteristics

Device [#]	Type [#]	Sliding material	Req [m]	μ [#]	Number of Sliding surfaces
1	1	Filled PTFE	3.0	0.05	Double
2		ULDPE		0.03	Double
3		Vergin PTFE		0.01	Double
4	2	PTFE based material	3.0	0.05	Single
5			5.5		Double
6			4.2		Single



The six devices are grouped by type as follows:

- Type #1: the stainless steel sliding surface is installed into a counterbore of the housing plate, thus a gap is originated between the sliding interface and the outer rim of the plate;
- Type #2: the stainless steel sliding surface is installed by means of a weld bead, so that a unique solid element is created, and no replacement of the sliding interface is generally possible.

The difference between Type #1 and Type #2 devices is schematically outlined in Fig. 1. In both cases, the sliding pad can travel passed the design displacement (i.e. the nominal capacity) of the device. However, some extent of damage to the slider is expected to occur on the loading cycle for Type #1 bearings, and on the returning cycle for Type #2 bearings.

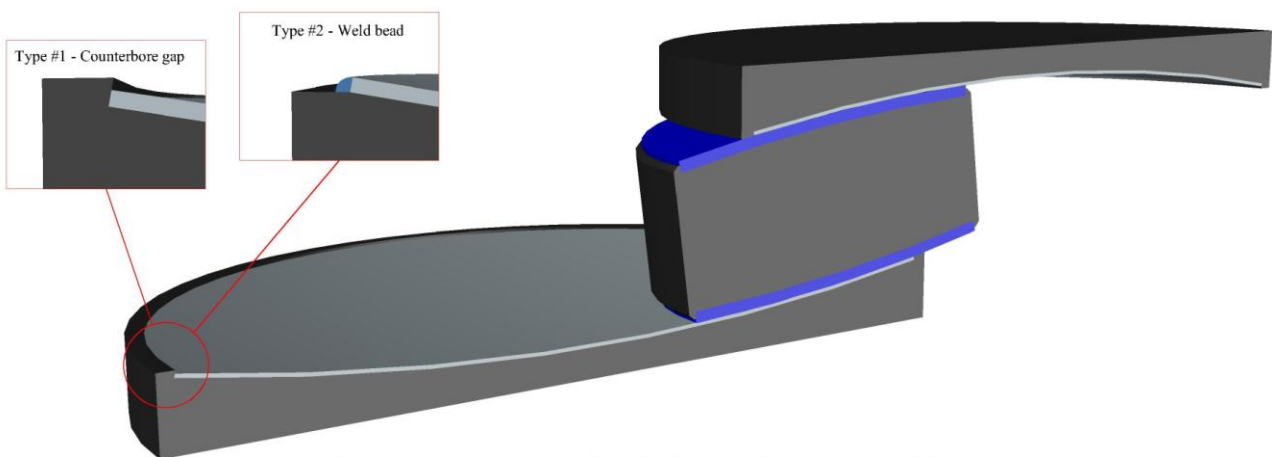


Fig. 1 – Example of tested device typologies

3. Testing protocol

Quasi-static and dynamic tests were performed considering triangular and sinusoidal forces, as shown in Fig. 2. Table 2 provides the summary of the test protocols.

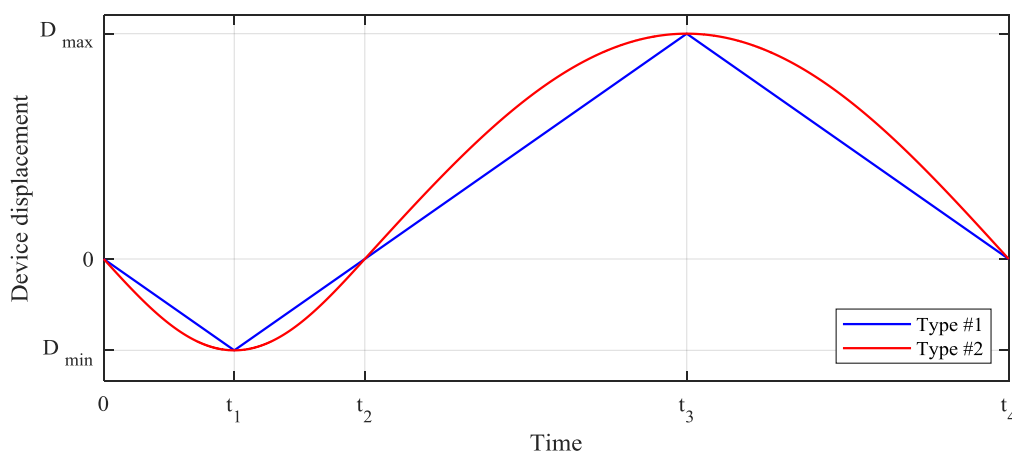


Fig. 2 – General waveforms used for tests



It should be noted that Type #2 devices achieved much higher peak velocities, even though the peak value V_{\max} is reached at just a single time instant, whereas the triangular waveform has constant velocity values.

Table 2 – Testing protocol

Device [#]	Type [#]	Waveform	D_{\max}/D_d [#]	V_{\max} [mm/s]
1	1	Triangular	1.52	2.5
2			1.52	2.5
3			1.52	2.5
4	2	Sine	1.28	15.0
5			1.27	15.0
6			1.29	15.0

The maximum displacement demand D_{\max} of each test was computed considering a displaced configuration of the device with 25% of the inner pad uncovered by the sliding interface for vertical stability. When DCSS devices are used, higher displacement demands can be achieved because two sliding surfaces are engaged.

4. Experimental results

The hysteretic responses of all Type #1 devices are reported in Fig. 3. Both horizontal forces and displacements are normalized with respect to the design values. It can be seen that passed the nominal capacity, the response experiences an initial smooth increase in stiffness (over a short distance), followed by stiffness “stabilization” at a value which is very close to the expected restoring stiffness of the device, computed as the ratio between the applied vertical load and the equivalent radius of curvature.

It should be noted that at the end of all the tests on Type #1 devices, the sliding material presented significant damage, with large portions of the low-friction material detached from the slider (see Fig. 6).

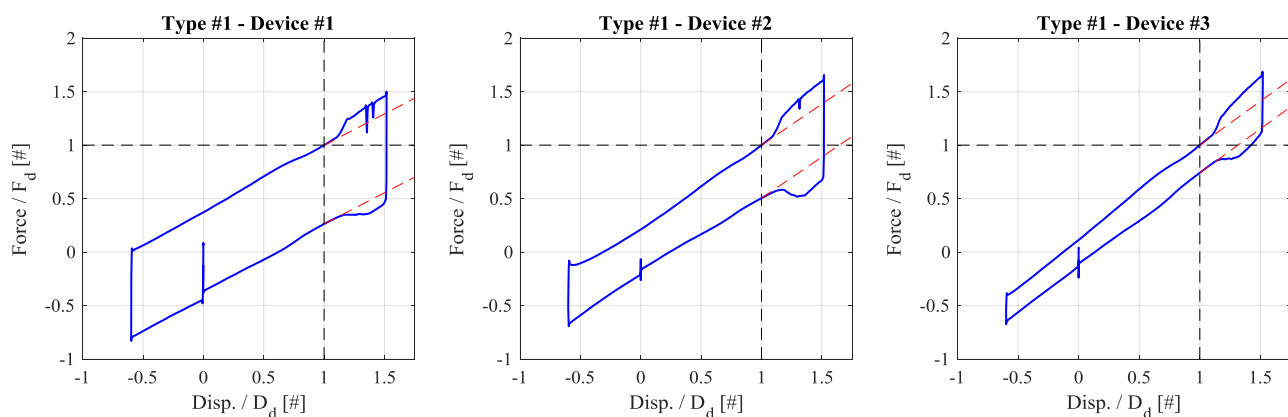


Fig. 3 – Results: Normalized hysteretic loops (Devices type #1)

The results summarized in Fig. 3 suggest that exceeding the design displacement of the device leads to an increase of the friction coefficient, if the stainless steel sliding surface is installed into a counterbore gap. In order to better highlight such aspect of the response, the “pure friction” behavior of the devices was isolated, by subtracting the re-centering force (modeled linearly with respect to the applied displacement time series) from the total force of the devices. The normalized response of the devices attributed solely to friction is shown in Fig. 4. In all cases the responses are approximately symmetric with respect to the displacement-axis, suggesting that the same friction coefficient is mobilized upon loading and unloading. Interestingly, the



friction coefficient increased by 33% for Device #1 (nominal value 5%), and by 100% for both Devices #2 and #3 (nominal friction values 3% and 1%, respectively).

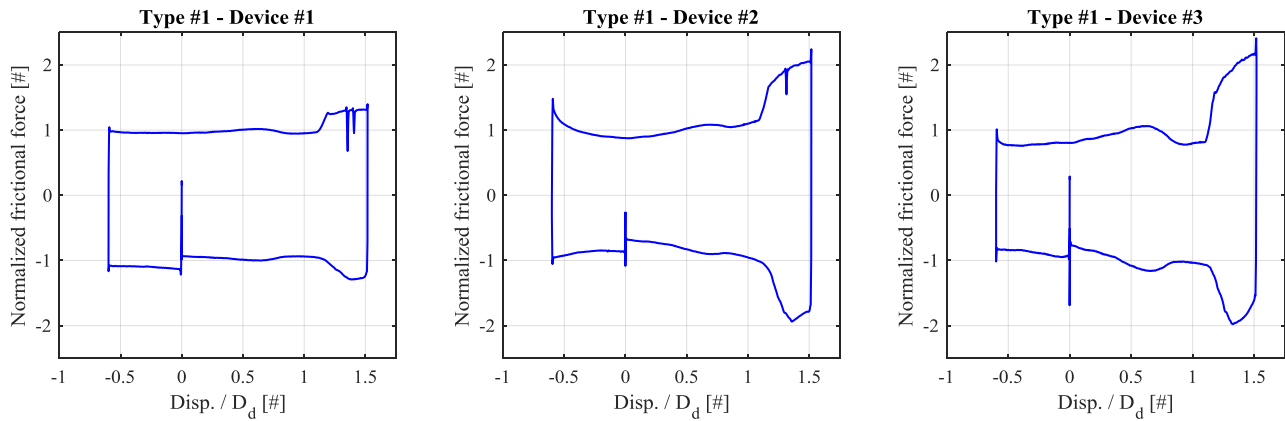


Fig. 4 – Results: normalized frictional responses

The hysteretic responses obtained for all Type #2 devices are presented in Fig. 5. Unlike what seen for the Type #1 devices, no significant variation in the “post-design” force-displacement response can be detected for devices #4, #5 and #6. To this end, it can be seen that their tangent stiffness remains essentially constant and very close to the elastic stiffness value estimated from the pendulum motion. Hence, it appears that when the inner slider exceeds the nominal displacement capacity of Type #2 devices, “ordinary” response of the CSS device is to be expected at all displacement levels. This is because the weld bead provides a smooth transition of the sliding motion at the maximum deformation allowance, with negligible damage of the sliding material.

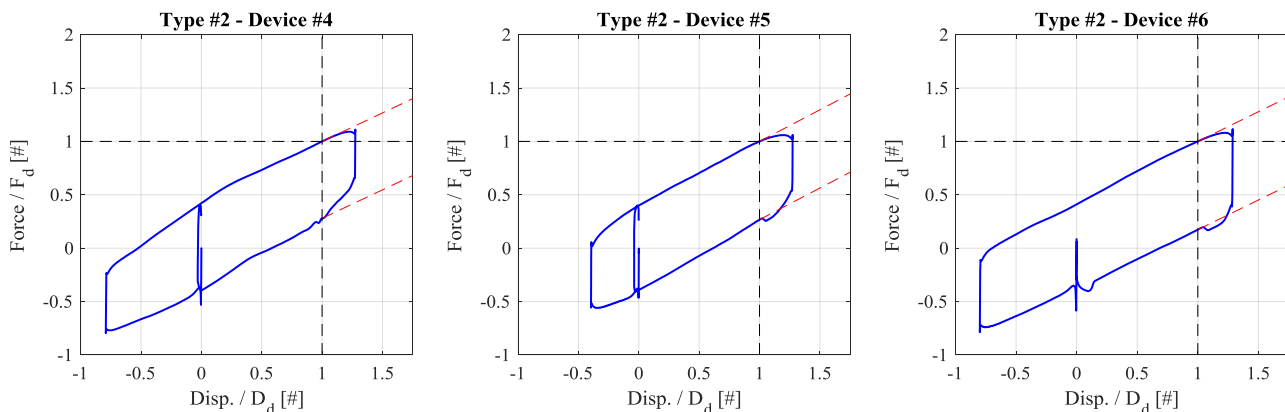


Fig. 5 – Results: Normalized hysteretic loops (Devices type #2)

Fig. 6 provides a view of the status of the sliding pads at the end of each test. As anticipated, different extent of damage was detected for Type #1 and Type #2 devices. More specifically, significant damage of the slider can be observed pertaining to all Type #1 devices, whereas the damage is very limited for the Type #2 devices. The greater extent of damage detected for the Type #1 specimens was attributed to the presence of the counterbore gap, which contributed to cutting and slicing portions of the sliding material. However, for



both the isolation typologies studied, the overall force-displacement responses appeared stable at all displacement levels.

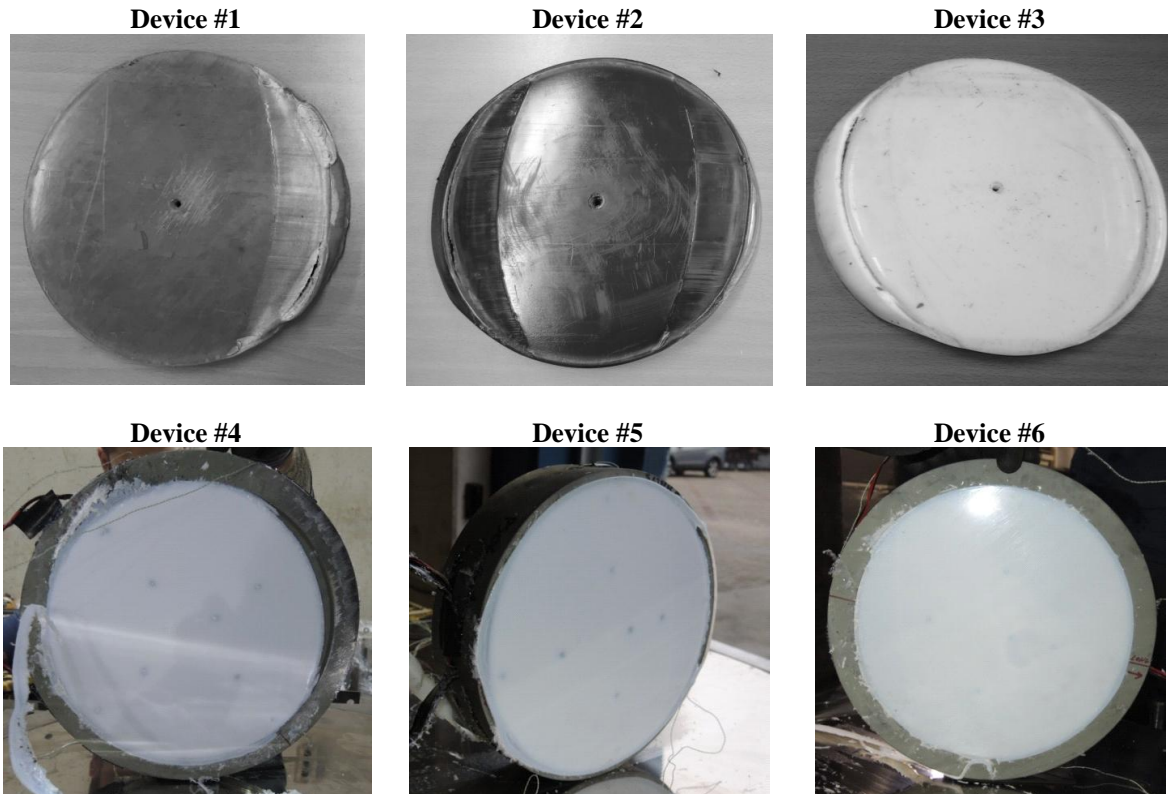


Fig. 6 – Damaged sliding pads

5. Discussion & modeling strategies

The preliminary results presented in the previous sections are promising and suggest that the typologies of CSS devices considered in this study may be capable of achieving higher displacements than the maximum geometrical allowance (i.e. the nominal capacity). Ideally, this extra displacement capacity should be considered in design/assessment and a new definition of “collapse” should be introduced for these sliding isolators, corresponding to the loss of vertical bearing capacity. Theoretically, this loss occurs when the horizontal displacement leads to 50% of covered area of the sliding pad(s), which corresponds to a nontrivial increase in displacement capacity.

From a numerical modeling standpoint, the Type #2 devices considered in the experimental program presented in this paper can be modeled as traditional Friction Pendulum or Double Friction Pendulum systems, because their response is unaffected by the sliding pad exceeding the nominal displacement capacity of the isolator. However, Type #1 devices present a variation in the force-displacement response, which can be associated to an increased value of friction coefficient for both positive and negative directions of motion. While there are multiple ways of addressing this aspect in a numerical model, one simple approach that is suitable in the context of 1D motions is to use a properly calibrated empirical equation that describes the friction coefficient across the sliding surface of the device. Thus, the following analytical expression can be employed (eq. (1)):



$$\frac{\mu}{\mu_o} = p + \frac{\alpha}{2} \cdot \left[1 + \tanh\left(\frac{D - D_o}{U}\right) \right] \quad (1)$$

Being:

- μ : stepwise value of friction coefficient;
- μ_o : nominal value of friction coefficient;
- p : initial percentage of the friction coefficient in the ordinary sliding phase (to be set equal to 100%)
- α : variation percentage of the friction coefficient in the extra-displacement capacity
- D : stepwise value of displacement;
- D_o : Design value of displacement

Fig. 7 shows a qualitative graphic representation of the analytical expression of the shear force as a function of the displacement (eq. (1)).

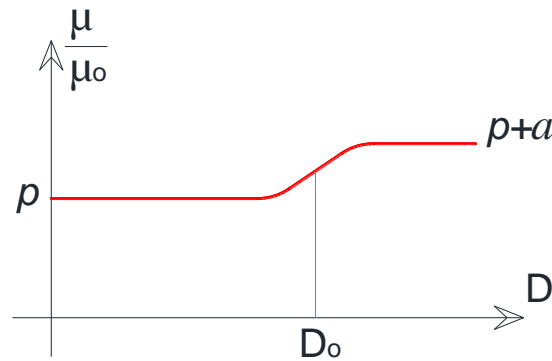


Fig. 7 – Frictional response analytical model

The empirical parameters in eq. (1) were calibrated based on the results of the experiments discussed in this paper. Comparisons between the experimental force-displacement hysteresis and the force-displacement responses obtained using the calibrated empirical approach are shown in Fig. 8.

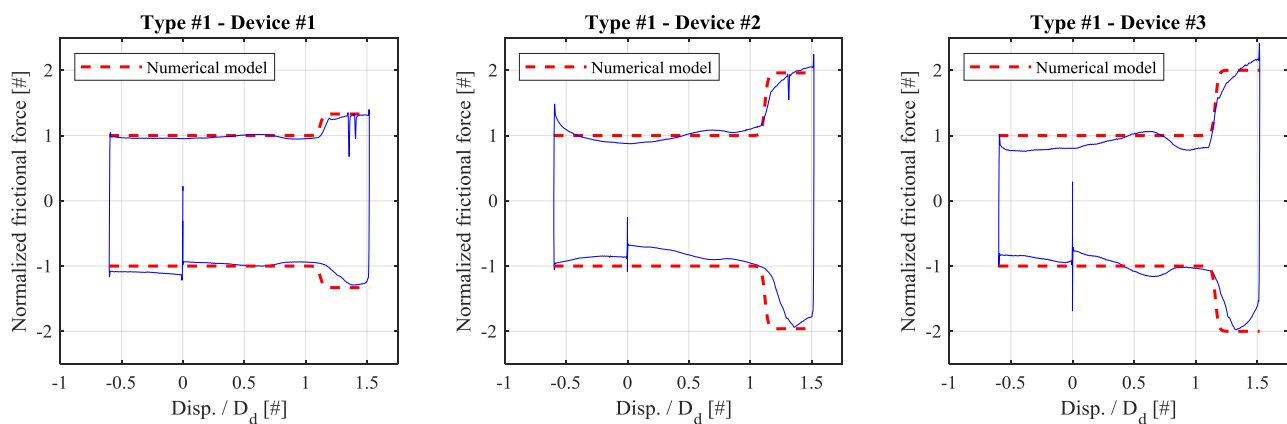


Fig. 8 – Frictional response analytical simulation (Devices type #1)

While further validation and refinement may be required, the analytical approach proposed in this section may be used to model the response of Type #1 CSS devices subjected to severe ground motions, thus



experiencing horizontal displacements that exceed their nominal capacity. In particular, the modeling approach described herein may be used in the context of preliminary 1D Non-Linear Time History Analyses (NLTHA), to assess the performance and vulnerability of structures isolated using this kind of devices.

6. Concluding remarks

This paper summarized the main results of an experimental program carried out at the EUCENTRE Foundation Laboratory (Italy). The objective of the study was to investigate the response of Curved Surface Slider devices under displacement demands that exceeded the design displacement. Quasi-static test and dynamic tests were conducted on several full-scale devices. The key findings of this research can be summarized as follows:

- Curved Surface Slider devices without restraining rims can achieve displacements that exceed the design values, without evident negative effects on the force-displacement response and the re-centering properties;
- When the stainless steel sliding surface is installed with a counterbore gap, a force increase (attributed to higher friction) is seen as the sliding pad exceeds the design displacement;
- When the sliding interface is installed with a weld bead on the backing plate of the device, the sliding pad can slide the design displacement with no significant variation in the force-displacement response;
- Reaching design displacement does not represent the failure condition of the isolation devices. Extra displacement capacity may be considered when designing/assessing these devices, depending on both the actual size of the sliding pads and the number of sliding surfaces;
- In case of counterbore gap technology, it is possible to model the extra displacement behavior by implementing a simple analytical expression, which captures the higher friction coefficient that arises when the design displacement is exceeded.

7. Acknowledgments

Part of the current work has been carried out under the financial support of the Italian Civil Protection, within the frameworks of the Executive Project 2017–2019 (Project 3 – Assessment of the seismic isolation of building structures through hybrid tests with numerical substructuring) and the national Research Project DPC – ReLUIS (National Network of Laboratories of Seismic Engineering) 2014–2018, Line 6 – Isolation and Dissipation.

8. References

- [1] Bao Y., Becker T.C., Sone T., Hamaguchi H. (2017) Experimental study of the effect of restraining rim design on the extreme behavior of pendulum sliding bearings. *Earthquake Engineering and Structural Dynamics*, DOI: 10.1002/eqe.2997.
- [2] Barone S., Pavese A., Calvi G.M. (2017) Experimental dynamic response of spherical friction-based isolation devices. *Journal of Earthquake Engineering*, DOI: 10.1080/13632469.2017.1387201.



- [3] Calvi P.M, Calvi G.M. (2018) Historical development of friction-based seismic isolation systems. *Soil Dynamics and Earthquake Engineering* 106(2018):14-30.
- [4] Cardone D., Conte N., Dall'Asta A, Di Cesare A., Flora A., Lamarucciola F., Micozzi F., Ponzo F.C., Ragni L. [2019], "RINTC_E Project: the Seismic Risk of Existing Italian RC Buildings Retrofitted with Seismic Isolation", *COMPDYN 2019, 7th ECCOMAS Thematic Conference on Computational Methods in Structural Dynamics and Earthquake Engineering*, Crete, Greece, 24–26 June 2019.
- [5] Dolce M., Cardone D., Croatto F. (2005) Frictional behavior of steel-PTFE interfaces for seismic isolation. *Bulletin of Earthquake Engineering*, 3, 75–99.
- [6] Eurocode 8 Design of structures for earthquake resistance Part 1: General rules, seismic actions and rules for building; UNI EN 1998-1.
- [7] Fenz D., Constantinou M.C., Behaviour of the double concave friction pendulum bearing. *Earthquake Engineering And Structural Dynamics*, 35,1403–1424, 2006.
- [8] Furinghetti M., Pavese A., Quaglini V, Dubini P (2019) Experimental Investigation Of The Cyclic Response Of Double Curved Surface Sliders Subjected To Radial And Bidirectional Sliding Motions. *Soil Dynamics and Earthquake Engineering*, DOI: 10.1016/j.soildyn.2018.11.020.
- [9] Furinghetti M., Pavese A. (2019) Assessment of the Seismic Response of Isolated Bridges under extra-stroke displacement demands. 41th IABSE Symposium, March 27-29, 2019, Guimarães, Portugal.
- [10] Kumar M., Whittaker A.S., Constantinou MC (2015) Characterizing friction in sliding isolation bearings. *Earthquake Engineering and Structural Dynamics*, 44,1409–1425.
- [11] Mazza F., Mazza M. (2017) Sensitivity to modelling and design of curved surface sliding bearings in the nonlinear seismic analysis of base-isolated r.c. framed buildings. *Soil Dynamics and Earthquake Engineering*, 79, 951-970.
- [12] Pavese, A., Furinghetti, M., Casarotti, C. (2018) Experimental Assessment of the Cyclic Response of Friction-Based Isolators under Bidirectional Motions. *Soil Dynamics and Earthquake Engineering*, DOI: 10.1016/j.soildyn.2018.06.031.
- [13] Peloso, S., Pavese, A., Casarotti, C. [2012] "Eucentre trees lab: Laboratory for training and research in earthquake engineering and seismology," *Geotechnical, Geological and Earthquake Engineering*, Vol. 20, pp. 65-81.